Science of the Total Environment 951 (2024) 175756

Contents lists available at ScienceDirect

Science of the Total Environment

journal homepage: www.elsevier.com/locate/scitotenv

Future climate change and marine heatwaves - Projected impact on key habitats for herring reproduction

Matthias Gröger [a,*], Florian Börgel [a], Sven Karsten [a], H.E. Markus Meier [a], Kseniia Safonova [a], Cyril Dutheil [b], Aurore Receveur [c], Patrick Polte [d]

[a] Department of Physical Oceanography and Instrumentation, Leibniz Institute for Baltic Sea Research Warnemünde, Seestraße 15, 181 19 Rostock, Germany
[b] MARBEC, University of Montpellier, CNRS, Ifremer, IRD, Sète, Montpellier, France
[c] FRB-CESAB, 5 Rue de l'École de Médecine, 34000 Montpellier, France
[d] Thuenen Institute of Baltic Sea Fisheries, Alter Hafen Süd 2, 180 69 Rostock, Germany

HIGHLIGHTS

- The number of MHW days ~triples under the 1.5 °C global target and further increases at a rate of 36 to 48 days yr^{-1}/0.5°C beyond the 1.5 °C target
- Phenological winter duration is reduced by ~25% even in the 2.0°C target but reduces up to ~60% in the 4.0°C scenario compared to the historical climate and more winters miss completely
- Herring larvae will face more frequent days with heat stress inducing cardiac dysfunctions
- Abiotic disturbances for the Baltic Sea marine ecosystem can be at least partly mitigated if global warming remains below or compliant with the 1.5°C target

GRAPHICAL ABSTRACT

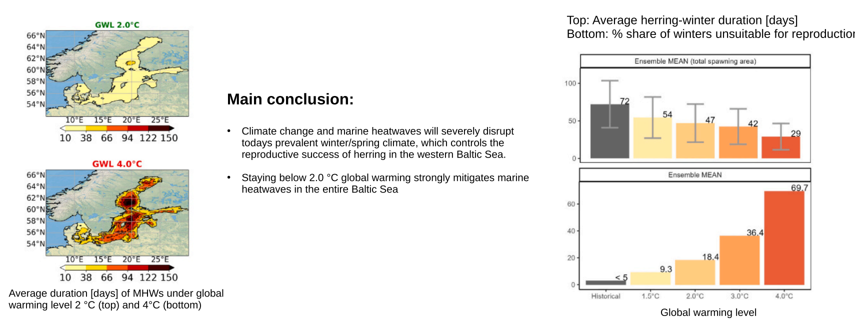

ARTICLE INFO

Editor: Julian Blasco

Keywords:
Climate change
Regional climate impact
Fish habitats
Marine heatwaves

ABSTRACT

This study explores the impact of global climate targets on sea surface temperatures and marine heatwaves (MHWs) in the Baltic Sea. We further evaluate potential adverse climate effects on the reproductive success of the western Baltic Sea (WBS) herring stock, which underwent a dramatic decline during the past two decades. For this, we use refined ensemble climate projections from the Coupled Model Intercomparison Project. For the WBS herring spawning ground, the number of MHW days nearly triples from 34 days/year in the historical period, to 102 days/year already under the optimistic 1.5 °C target of global climate warming (Paris, 2015) and further increases at a rate of 36 to 48 [days yr^{-1}]/0.5 °C beyond the 1.5 °C target. The average MHW surface extent more than doubles in the 1.5 °C target from ~8 % to 21 % in this area.

This study finds the phenological winter climate considerably altered in response to future global warming and more frequent MHW days in the WBS. The winter duration reduces by ~25 % already in the 2.0 °C target but by ~60 % in the 4.0 °C target compared to the historical climate. Winter inceptions/terminations occur successively later/earlier and the share of missed winters, i.e. winters unsuitable to support herring reproductive success, increases by up to ~70 %. Days with heat stress on the cardiac function of herring larvae will likewise increase

* Corresponding author.
E-mail address: matthias.groeger@io-warnemuende.de (M. Gröger).

https://doi.org/10.1016/j.scitotenv.2024.175756
Received 21 March 2024; Received in revised form 23 July 2024; Accepted 22 August 2024
Available online 23 August 2024

and occur earlier in the year. Consequently, the early life cycle of herring will face more often winter conditions that were unprecedented during the historical past, and the risk for future reproductive failure will increase. However, our results reveal that abiotic disturbances for the marine ecosystem can be partly mitigated if global warming remains compliant with the 1.5 °C target.

1. Introduction

The Paris Agreement (PA) of the United Nations Framework Convention on Climate Change (UNFCCC, 2015) aims to keep global climate warming well below 1.5 °C or 2.0 °C above the preindustrial level. However, even under these strongly mitigated scenarios, the regional climate impact can still be substantial and thus require further local-specific actions to sustain ecosystem services. The Baltic Sea hosts one of the Worlds' most vulnerable marine ecosystems (Kuliński et al., 2022; Viitasalo and Bonsdorff, 2022) and belongs to the most intensively exploited shelf seas (Reckermann et al., 2022). At the same time it is among the fastest warming marginal seas of the World ocean (Christensen et al., 2022; Meier et al., 2022a, 2022b) with a long term warming of 0.06 °C/decade since 1850 (Dutheil et al., 2022, 2023). Moreover, as consistently revealed by hindcast simulations for the historical and present climate, warming trends of extreme surface water temperatures are between 30 and 70 % higher than trends in annual mean temperatures (Gröger et al., 2022). Future climate simulations for the Baltic Sea project a warming of the mean sea surface temperature between 1.7 and 3.3 °C at the end of the 21st century depending on the season and the greenhouse gas scenario (Saraiva et al., 2019; Gröger et al., 2019; Meier et al., 2022b). Due to its strong sensitivity to climate warming, the Baltic Sea was already subject to an increasing number of marine heatwaves (MHW, hereafter) in the historical period (Goebeler et al., 2022; Gröger et al., 2022; Gröger et al., 2024; Meier et al., 2022b).

In the Baltic Sea high freshwater input by river runoff in combination with restricted inflow of marine water through the narrow channels (max. 200 m width) from the North Sea, form a perennial halocline that effectively hampers vertical ventilation. This limits the upper ocean mixed layer and thus, lowers the effective heat inventory prone to atmosphere-ocean heat exchange. As a consequence, the Baltic Sea is very sensitive to global warming (Meier et al., 2022b) and so the effects of climate change and MHW can be explored early. MHWs in the Baltic Sea are clearly meteorologically forced and were linked to two characteristic large-scale atmospheric weather regimes (Gröger et al., 2024). Accordingly, stable Scandinavian blocking patterns, i.e. long lasting high pressure systems, drive an anomalous high radiative heat absorption during summer. During winter a large-scale pattern of elevated meridional sea level pressure gradients over the North Atlantic drives an anomalous strong advection of warm air masses to the Baltic Sea region thereby effectively reducing the ocean heat flux out of the upper halocline layer (Gröger et al., 2024).

The sensitivity of the Baltic Sea to global warming stimulated the discussion about the existence of tipping points for the Baltic marine ecosystem and whether these could be irreversibly crossed in the cause of ongoing future climate warming (Möllmann et al., 2021; Receveur et al., 2022). Coastal herring habitats are mainly threatened by eutrophication, pollution, coastal modification, species introduction, and climate change (Fey et al., 2014). Climate change directly influences abiotic stressors such as temperature, salinity and oxygen contents. However, direct links between climate change and discrete ecological effects have not yet identified but rely mostly on statistically derived relationships rather than on direct empirical evidence (Polte et al., 2021; Receveur et al., 2022). At the same time the Baltic sea is intensively exploited by the fishery industry of the nine Baltic Sea neighboring countries. Actually, two economically important fish stocks, i.e. the herring and cod populations (Polte et al., 2021; Möllmann et al., 2021) in the Western Baltic Sea (WBS hereafter) experienced a dramatic diminishing. For example, the WBS herring spawning stock biomass reduced from ~300.000 t in the year 1990 to ~50.000 t in 2020 and fish catches reduced from almost 200.000 t to roughly 25.000 t in parallel (Moyano et al., 2023). The WBS herring stock is one of the most important economic resources for the marine food production in the Baltic Sea. Both the spawning biomass, and the recruitment of herring underwent a substantial decrease in the Baltic Sea during last two decades (Receveur et al., 2022). This repeatedly stimulated the controversial debate on quotas among the EU fisheries ministers to protect the herring population to collapse. While industrial fishing is considered the most important driver to manage the herring resources in the Baltic Sea, it has recently been suggested that climate warming may threaten the WBS herring stock by diminishing its reproductive success (e.g. Moyano et al., 2020; Polte et al., 2021).

The dramatic decline of the herring stock was paralleled by a clear decline in offspring year-classes. Early observations pointed to the predominant winter regime as pacemaker for the reproductive success (Gröger et al., 2014). More recently, Polte et al. (2021) demonstrated the herring decline during the last decades strongly correlated with simultaneous changes in winter timing. More precisely, winter inception and termination explained much of the variability in recruitment. In their study, the winter season was defined based on the water temperature thresholds that enables initial spawning (Initial Spawning temperature, ISP). A late winter inception and/or early termination was found to negatively impact on herring recruitment. The exact mechanism is still unclear but the authors hypothesized a temporal mismatch of hatched herring larvae and their prey as main reason.

Independent from exact mechanisms it must be expected that climate change will influence the timing of inceptions and terminations of future winters. Hence, climate model projections can be used to investigate future changes in abiotic drivers of winter phenology and thus provide valuable information on the climate induced stress on the herring's reproductive success. Moreover, even under moderate climate warming, we hypothesize, the occurrence of MHWs can significantly shift the winter timing in individual years with potentially longer lasting effects on the herring reproduction. Consequently, in this study we also investigate how MHWs affect the winter phenology of the early herring life cycle.

Overall, this study addresses two relevant climate change related issues in the Baltic Sea. 1) The effectiveness of the PA is assessed with regard to the mean climate change and to MHWs. This is done for the entire Baltic Sea to provide basic knowledge for the ongoing marine spatial planning of marine protected areas. Climate change and recently MHWs are considered an increasing pressure in the Baltic Sea which potentially disturb the operation of MPAs. Therefore, climate change and MHWs were recently suggested to be considered in the planning of MPAs (Safonova et al., 2024). 2) The potential effect of climate warming and MHWs is assessed for the reproductive success of the WBS herring stock. This is addressed by future displacements of winter timing and by the projected increase of days with disturbances in the cardiac rhythm of herring larvae. Thus, this study combines the recent findings on key herring phenological parameters (Moyano et al., 2020; Polte et al., 2021) with climate change information from state of the art climate projections for the Baltic Sea.

2. Methods

2.1. Regional climate model ensemble

The ocean climate ensemble used in this study was produced by the

Rossby-Center Ocean general circulation model RCO (Meier et al., 2021). This model was driven with atmospheric output from 4 global climate models from the Coupled Model Intercomparison Project phase 5 (CMIP5), that were downscaled with a regional coupled ocean atmospheric model (Dieterich et al., 2019). RCO has a horizontal resolution of ~3.5 km and resolves the water column by 83 vertical z-levels. Unlike global ocean models which are designed to reproduce the large scale circulation of the World Ocean, RCO allows to resolve mesoscale variability and small-scale topographic features of the Baltic Sea. RCO is an established ocean climate model that was used in numerous climate change studies for the Baltic Sea (e.g. Meier et al., 2021, 2022b, and references therein). A complete scheme for the data production and processing is provided in the Suppl. Mat. S0. Please note the downscaling experiments with RCO started in 1961 and run until 2100. However, the first 15 years were not analyzed to avoid spin up effects of the model. More information about the RCO ocean model, the downscaling procedure, and the model validation is available from the literature (e.g. Saraiva et al., 2018, 2019; Placke et al., 2018; Meier et al., 2021, 2022a).

The here employed greenhouse gas scenarios follow the Representative Concentration Pathway (RCP) scenario RCP8.5 (described in Moss et al., 2010). This high end emission scenario is selected in order to reach also the extreme global warming level of +4 °C compared to the preindustrial level (Table 1).

In order to define reference climatologies compliant with the Paris targets of global mean warming relative to the preindustrial climate, we follow the established method by Kjellström et al. (2018). Accordingly, we analyzed the global climate models' annual mean air temperatures 2 m above ground (T2m). Global mean warming levels (GWL hereafter) were then defined as 30 year periods centered around the first year that exceeded a GWL of 1.5 °C, 2.0 °C, 3.0 °C, and 4.0 °C (GWL1.5, GWL2.0, GWL3.0, and GWL4.0 hereafter) respectively above the preindustrial T2m level (Table 1). In line with the rapidly ongoing global climate change and the transient nature of CMIPs global model simulations the 30-year periods partly overlap between two successive GWLs (see Kjellström et al., 2018). The obtained 30 year periods were then used for the analysis of the Baltic Sea regional climate ensemble simulations which were started in 1975. In this study the climatological reference period is considered from 1976 to 2005 as the regional Baltic Sea simulations with RCO started in 1976. At this time observational evidence suggests the global warming was already ~1 °C warmer compared to the preindustrial temperature 1860–1890 (see Kjellström et al., 2018).

2.2. Marine heatwaves

MHW are defined and categorized after Hobday et al. (2016, 2018). This method defines a MHW when daily temperatures exceed the 90th percentile temperature of the climatological reference period 1976–2005 for at least 5 consecutive days. Interruptions up to two days were neglected. Besides this, the intensity of MHWs were categorized based on multiples of the difference between the daily 90th percentile and the daily mean of the reference period (Hobday et al., 2018). The exact procedure employed for this study is described in Gröger et al. (2024). The detection of future MHWs relies on the daily thresholds of the historical reference climatology, in order to consider the "total heat exposure" for marine ecosystems (Sen Gupta, 2023). For analysis, the following indices were calculated for every grid cell (varying between ~9.5 km^2 and 13,5 km^2) of the model and for each GWL separately:

MHW duration: denotes the average duration of MHW within a 30-year period around the GWL.
MHW days: denotes the total number of MHW days per year averaged over a 30-year period around the GWL.
MHW extent: denotes the yearly average MHW extent in the entire Baltic Sea at the seas surface.

In most cases the MHW indices are displayed and discussed as averages over 1) all grid cell of the WBS spawning grounds (Figure, right panel), and 2) as averages over the 30-year periods that correspond to respective GWL scenarios.

Table 1
Downscaled global models and years at which global warming levels were detected. Global warming levels (GWLs) were diagnosed based on the global mean 2 m air temperature anomalies compared to the preindustrial period 1850 to 1890 (Kjellström et al., 2018). Downscaling was done with the regional Baltic Sea model RCO (Meier et al., 2021). The historical period serves as reference to which future changes are calculated in this study because RCO-data are not available before 1976. Hence, for example climate changes corresponding to a GWL4.0 are therefore expressed as change between the 30-year assessment period centered around 1991, and the 30-year period when the driving global model has reached GWL4.0 (relative to the global models 1861–1890 period, Kjellström et al., 2018) which is 2075 in case of MPI-ESM, 2073 in case of EC-Earth, 2068 in case of IPSL-CMA5-MR, and 2073 in case of HadGEM2-ES.

Global model	Historical period	GWL1.5	GWL2.0	GWL3.0	GWL4.0
MPI-ESM-LR	1991	2015	2031	2056	2075
EC-Earth	1991	2020	2038	2060	2073
IPSL-CMA5-MR	1991	2016	2031	2051	2068
HadGEM2-ES	1991	2026	2037	2056	2073

2.3. Indices for herring environmental parameters

All indices of herring are based on absolute temperature threshold derived from empirical studies. Therefore, the temperature data of the model ensemble were treated with a simple bias correction (Suppl. Mat. S1) before the herring indices were calculated. Based on the recent field studies in the Greifswald Bay (Fig. 1, right) from Polte et al. (2021) and Moyano et al. (2020), we employ two temperature indices to infer changes in the timing of initial spawning temperature and for the cardiac functioning of herring larvae and its link to climate and MHW. Strictly speaking, these thresholds are confirmed only in the Greifswald Bay, but we assess the indices also for the other potential spawning grounds in the WBS (right map in Fig. 1) as it is reasonable to assume, that also in those locations the winter timing controls the phenological characteristics of early herring life stages even though the absolute threshold may be slightly different outside the Bay. However, we exclude the areas outside the WBS as these areas may encompass very different environmental settings compared to the Greifswald Bay in terms of temperature, salinity, light climate or seasonal ice cover. At least for the WBS as depicted in Fig. 1 (right panel) our analysis revealed spatially very homogenous results. The spawning areas are derived from the Helsinki Commissions (HELCOM) Map and Data Service (MADS, https://helcom.fi/baltic-sea-trends/data-maps/). According to MADS the herring spawning areas relate primarily to main habitat associations, based on existing observations of herring spawning grounds. High probability spawning areas are denoted when the photic zone overlaps with any of the considered habit associations. Further details are given in the Essential Fish Habitats map serve for herring spawning within the MADS (https://maps.helcom.fi/website/mapservice/?datasetID=bae53d8e-a5a2-4d01-b260-54d72ad46813).

2.3.1. Winter inception and termination

The prevailing winter regime was identified as main controlling factor for the reproductive success of the western Baltic herring stock (Polte et al., 2021). Deviating from the usual meteorological definition, the winter season was determined based on the empirically derived relationship between initial spawning and water temperature (Polte et al., 2021). More precisely, the onset of the winter season was determined relative to the 22 September (autumn equinox) as the day when the water temperature falls below 3.5 °C for seven consecutive days (i.e. the lower limit of the initial spawning range of 4.0 ± 0.5 °C found by Polte et al., 2021). The arbitrarily chosen 22 September is taken as

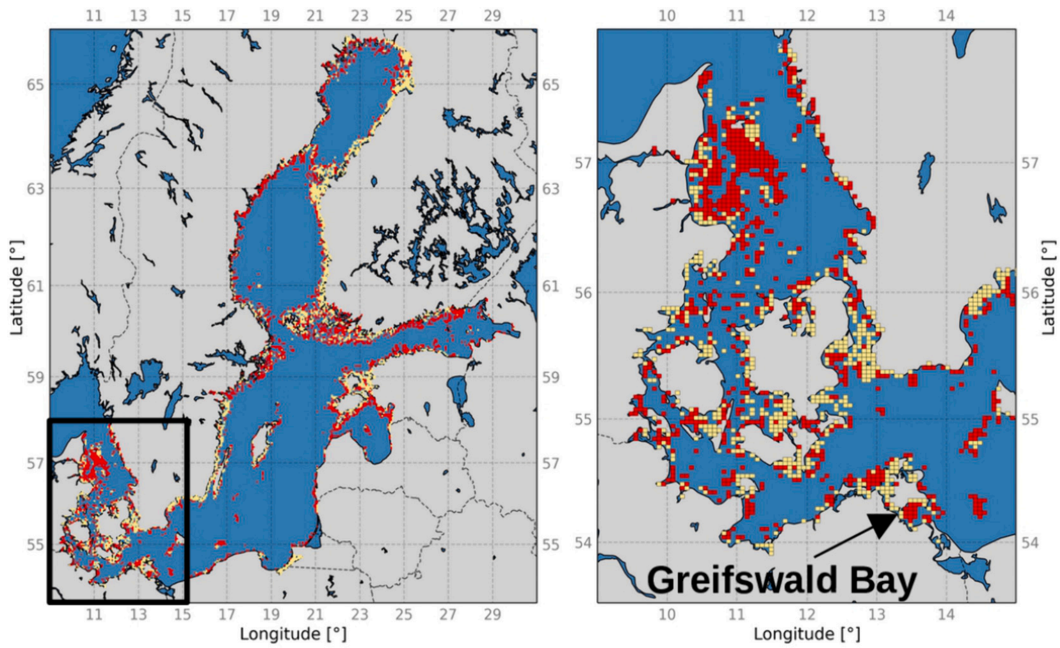

Fig. 1. Left: Map of the Baltic Sea model domain RCO. The colored grid cells indicate spawning locations derived from HELCOM. Right: Western Baltic Sea spawning area which is used to calculate herring indices. Yellow = potential spawning areas. Red = high probability spawning areas. Note, in this study no distinction between high and lower probability areas was done. The black rectangle in the left panel indicates the zoom area focused in the right panel.

reference to be consistent with the study of Polte et al. (2021) which ensures that any inception/termination can be expressed as positive value (since SST never fall below 3.5 °C at or before this date). Likewise, the end of the winter season was defined as day when the temperature ascends again above 3.5 °C. The time period between these two days determined the length of the winter season. In particular, a late winter inception together with a short winter duration was found to diminish the success of herring reproduction (Polte et al., 2021).

2.3.2. Separating the effect of MHW on inceptions/terminations compared to normal conditions

The Baltic Sea SSTs have a large inter-annual variability owing to different phases of the North Atlantic Oscillation (NAO). One aim of the study is to distinguish the effect of MHWs on winter inception and termination compared to normal conditions, i.e. without MHWs. Therefore, we compare the probability distributions for terminations and inceptions that occur under MHWs and normal conditions. Below the procedure for winter inceptions is outlined. The same procedure is applied for terminations.

This procedure is applied separately for all grid cells located in the WBS spawning grounds (Fig. 1, right), for each 30-year GWL and for each model. First, for all years without a marine heatwave during the inception, we calculate the difference between the inception day (relative to the fall equinox, Polte et al., 2021) and the average of all inception days (with and without MHWs), given the inception deviation for normal conditions. A similar difference is calculated between each year with a marine heatwave during the inception day and the average of all inception days (with and without MHWs), given the inception deviation for MHWs conditions. Then, empirical probability distribution histograms were calculated indicating the number of inceptions (sum of inceptions over all grid cells belonging to the spawning grounds) on the y-axis with an increment of 5 days for x-axis.

An inception/termination was considered MHW related when the seven days before the incident were MHW days. As this procedure was done separately for each GWLs and models we can compare the MHWs effect among all GWLs and models. This was necessary as, in particular for the historical period and lower GWL scenarios, the number MHW related inceptions was too low for a robust estimation of the MHW effect.

2.3.3. Thermal threshold index

Physiological experiments by Moyano et al. (2020) indicate water temperatures above 16 °C as arrhythmia-inducing for the cardiac functioning of herring larvae. The authors introduced the thermal threshold index (THI hereafter) as number of days above the 16 °C threshold during the months March to June when the majority of larvae hatches.

3. Results and discussion

3.1. Projected mean warming in GWL scenarios

We here only briefly describe the response of SSTs to different GWLs to assess the effectiveness of the PA. The SST response to at the end of the century has already been analyzed in detail (Meier et al., 2022b). The SST response is spatially fairly homogenous (Suppl. Mat. S2) which is consistent with the small size of Baltic Sea and the large-scale meteorological forcing of the warming. Overall, the southwestern Baltic Sea warms slightly less compared to the northern regions (with exception of seasonally ice covered areas). The same is true for the shallow areas along the coasts. However, the strong efficiency of mitigation efforts of the PA is demonstrated. In the western Baltic Sea areas, the SST change remains below 1.3 °C in the GWL scenarios compliant with the PA. By contrast, at a GWL4.0 the SST change is almost everywhere higher than 2.5 °C. Averaged over the entire Baltic Sea the warming amounts to 0.89 °C, 1.27 °C 1.84 °C, and 2.76 °C for respectively for GWL1.5, GWL2.0, GWL3.0, and GWL4.0. The warming averaged over the WBS spawning grounds is in the same range with 0.83, 1.18, 1.7, and 2.57 corresponding to GWL1.5, GWL2.0 GWL3.0, and GWL4.0.

3.2. Projected surface extent of marine heatwaves

In a first step we assess the time-series of yearly mean MHW extent for the four models (Fig. 2). In the historical climate until 2005, MHWs almost never peaked above 100,000 km^2 but they increased in size to almost 400,000 km^2 (somewhat less in RCO-MPI-ESM) at the end of the century. Hence, even under high warming levels, MHWs do never cover

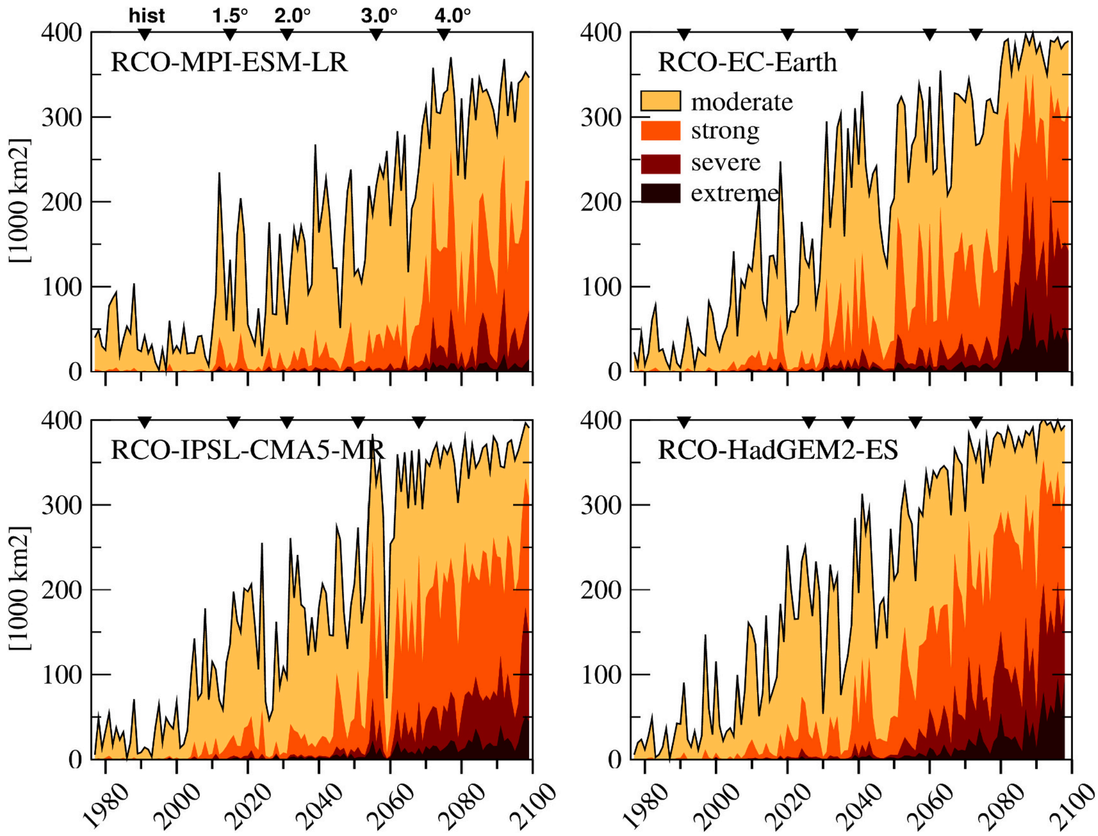

Fig. 2. Yearly mean surface extent of MHW in the Baltic Sea for the four models which were driven by the RCP85 scenario. Centers of 30 year periods for the historical period as well as for global warming levels relative to the preindustrial era are indicated by the triangles at the top of each panel.

entire the whole Baltic Sea (420,260 km^2) but maximal ~95 % of the sea surface in GWL4.0.

The MHW extent for the entire Baltic Sea and for the WBS spawning grounds is summarized in Fig. 3,e,f relative to corresponding the absolute total open sea (420,260 km^2) and total WBS spawning area (88,628 km^2, Fig. 1, right). Hence for the open sea the % share increases from 8.6 % in the historical period to successively, 25.5, 39.2, 59.2, and 77.4 % at the GWL1.5, GWL2.0, GWL3.0, and GWL4.0 respectively. In the WBS spawning ground, the increases are in the same range. Here, the % share increases from 8.7 % in the historical period to 23.2, 33.9, 52.4, and 72.5 % at a GWL of 1.5 °C, 2.0 °C, 3.0 °C, and 4.0 °C. Regarding the transient development, it is noteworthy that in all models category III (severe) or IV (extreme) MHWs reach the same extent (or even larger) at the end of the century as category I MHW (moderate) during the historical period (Fig. 2).

3.3. Projected duration of marine heatwaves

Besides their spatial extent and category, the duration is another significant measure to assess the MHW impact on the marine ecosystem (Chauhan et al., 2023; Rühmkorff et al., 2023). Fig. 4 shows the model ensemble averages corresponding to the considered GWLs. In the GWL4.0 scenario, the duration increases more strongly in the open sea areas compared to the coastal regions. This is likewise the case for the lower GWLs but masked in Fig. 4 where the scale is adapted to compare different GWLs. In any case, the coast – open sea contrast is most obvious for the 4.0 °C scenario when the inner basins turn into a permanent MHW state whereas coastal and shallow areas MHW are still frequently interrupted likely because they are more sensitive to meteorological variability on synoptical time scales. Hence, in the 4.0 °C scenario the average duration in the WBS spawning grounds is only ~55 days compared to ~73 days averaged the total Baltic Sea area (Fig. 3a, b).

The mitigation effect of PA compliant GWLs is obvious. Here, the average MHWs duration is more or less well below one month (Figure a, b). However, at GWL2.0 the average duration is already twice as long than in the historical reference period and in the GWL3.0 and GWL4.0 scenarios the duration rises to the ~3-fold and ~5-fold (4-fold in the WBS) compared to the historical period.

3.4. Projected increase of MHW days

So far our results reveal substantial changes in the future duration of MHWs which sooner or later will culminate in a more or less permanent MHW state. Hence, we here assess the total number MHW days per year rather than MHW frequency. For this, we calculated the MHW days index at GWL steps of 1.5 °C, 2.0 °C, 2.5 °C, 3.0 °C, 3.5 °C, and 4.0 °C, and calculated the increases per 0.5 °C global warming increments using a linear regression. The result is displayed for MHW categories I to IV and shows the increase of MHW days per year with every additional 0.5 °C global warming beyond the lower Paris target of 1.5 °C GWL (Fig. 5). MHW days of category I MHW increase between ~36–48 days per 0.5 °C warming. The spatial pattern is quite uniform and thus reflects the mean warming of the Baltic Sea water surface. In the Bothnian Bay north of 60°N the diminishing seasonal sea ice cover leads to more absorption of short wave radiation. As a consequence, the SST variability and the amplitude increases when the open sea water surface is not longer isolated by the ice sheet (Dutheil et al., 2022, 2023). This gives rise to more extreme SST conditions in that region.

For MHWs of category I, we found a strong effect already for the PA compliant GWLs. Hence for the whole Baltic Sea, MHW days increase from 31 days/year in the historical periods to successively, 107, 150, 212, and 284 days/year at the GWL1.5, GWL2.0, GWL3.0, and GWL4.0 (Figure c, d).

The response in the WBS grounds is only somewhat weaker (Fig. 3d).

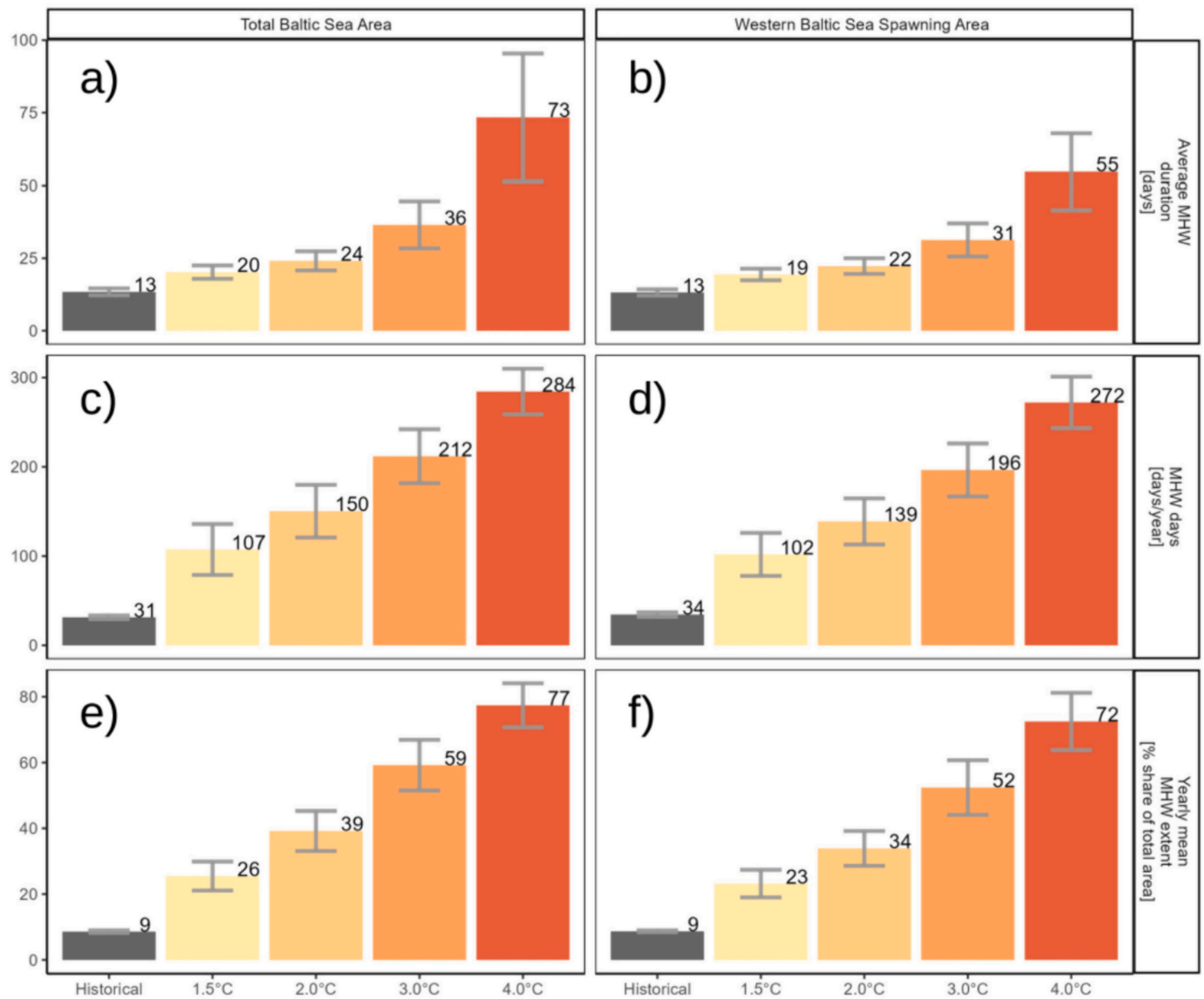

Fig. 3. Mean MHW statistics averaged over the whole Baltic Sea for the historical period and GWL targets. Numbers indicate the rounded values of the bars. Whiskers indicate the range of ensemble standard deviations. The left column displays statistics averaged over the entire Baltic Sea. The right column indicates value for the spawning grounds of the western Baltic Seas (Fig. 1, right).

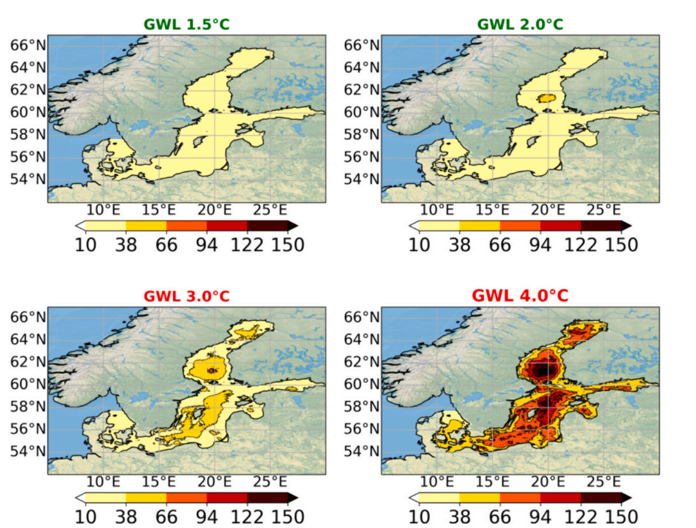

Fig. 4. Average duration [days] of MHWs under different global warming levels. Note MHW interrupted by maximal 2 days are considered as a single one.

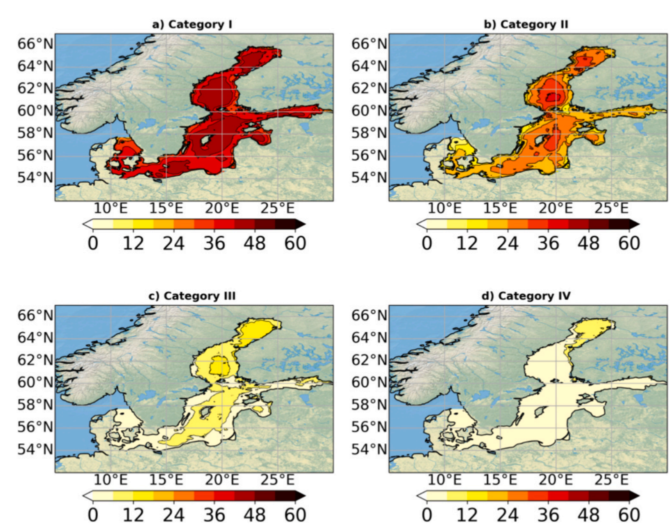

Fig. 5. Increase of MHW days per year and 0.5 °C GWL. a) Moderate MHW days, b) strong MHW days, c) severe MHW days, d) extreme MHW days.

Here, MHW days increase from 34 days/year in the historical period, to only 102, 139, 196, and 272 days/year at the GWL1.5, GWL2.0, GWL3.0, and GWL4.0.

3.5. Effect on herring phenology

In order to demonstrate the effect of climate warming on the winter termination and inception, we compare the historical period with the GWL4.0 scenario where the changes are most pronounced. It is obvious that climate warming substantially delays the winter inception and shifts the winter termination to earlier in the year (Suppl. Mat. S3). As a result the mean winter duration successively shortens in the GWLs from ~2 1/2 months in the historical climate to 1 month at GWL4.0 (Fig. 6, a). Apart from mean changes, the extremes can be challenging for the reproductive success. We thus calculated for each grid cell and each year the deviation of inception/termination from the respective climatological mean inception/termination GWL and evaluate the corresponding probability density distributions (Fig. 7). The most striking change between the historical period and GWL4.0 is the strong reduction in winters which is indicated by the diminished areas of the total distribution curves. Hence, in more and more areas the winter disappears, i.e. the temperature does not fall below the initial spawning temperature of 3.5 °C throughout the year. Such events are extremely rare in the historical periods but increases to 10 % and 18 % already at GWL1.5 and GWL2.0 (Fig. 6, d). With further warming, the share further doubles at GWL3.0 and quadruples at GWL4.0. Beside missed winters, extreme early termination/late inceptions are of particular interest, as they shift the timing of the winter and shorten the winter length. Though the climatological mean termination is moved by 2 weeks (from day 185 to day 170 after the equinox, or from the 24th to the 9th March, Fig. 6, c), both the extreme early and the extreme late terminations become more rare at GWL4.0 (tails of the density distributions, Fig. 7a, b) which is mainly the result of missed winters. However, the relative share of extreme early terminations (>1 month earlier than the average termination in the historical period = 24. March) increases substantially at GWL4.0: in the historical these extremes amount to only 16 % while at GWL4.0 the amount increases to 30 %. This relative increase is due to more frequent MHWs compared to normal conditions (Fig. 7a, b).

Also the climate induced delay of winter inceptions is evident in the density distributions (Fig. 7c, d). The upper quantile of the normal distribution is 10 days, i.e. only 20 % of inceptions are delayed by 10 days whereas at GWL4.0 20 % are delayed by 35 days. Inceptions directly

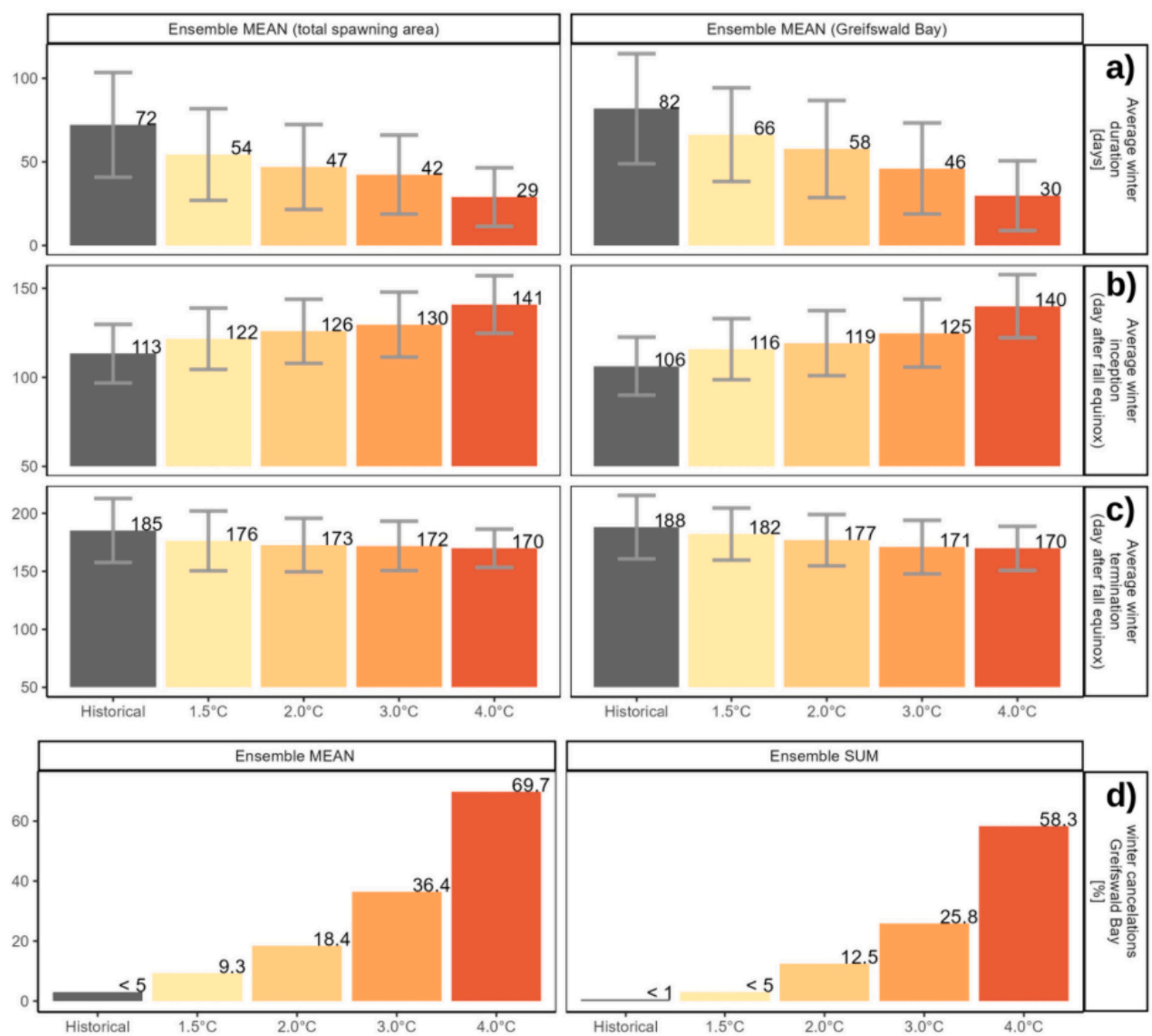

Fig. 6. Timing of a) winter duration, b) winter inception, and c) winter termination. Winter termination = days after the 22. September when the water temperature ascents above 3.5 °C for 7 consecutive days in spring. Winter inception = days after the 22. September when the water temperature falls below 3.5 °C for 7 consecutive days. The values are calculated as averages over time and spawning area for each model and each GWL scenario. d) Winter cancellations denote years in which the temperature never falls below 3.5 °C.

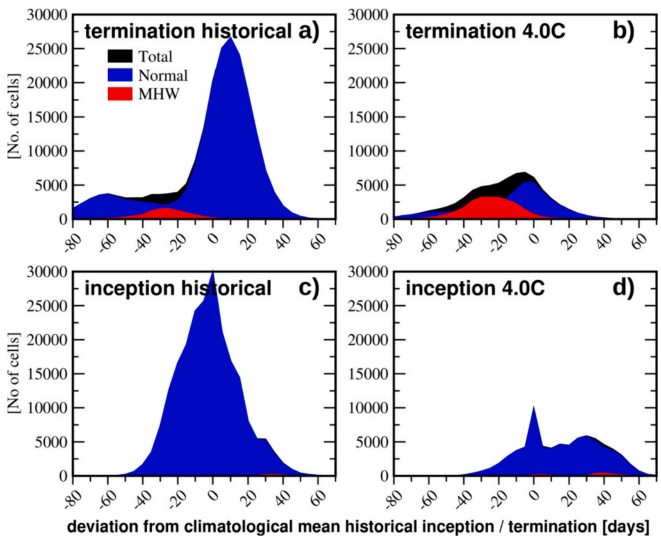

Fig. 7. Density distributions for termination (top row) and inception (bottom row) comparing the historical climate and the GWL4.0 scenario. The x-axis indicates the deviations from the climatological average day of inception (=13. January)/termination (=24. March) for the historical period/GWL4.0 scenario. The cumulative sum of the total distribution (black area) represents 100 %. The Normal distribution (blue) indicates the share of inceptions/terminations that were not preceded by a MHW over the 7 days before inception/termination at the given grid cell. The MHW distribution (red) indicates the share of inceptions/terminations that were preceded by a MHW over the 7 days before inception/termination at the given grid cell. Only grid cells were considered that belong to the WBS spawning grounds (Fig. 1, right).

induced by MHW are very rare. This is expected as MHWs directly tend to rise the temperature rather than pushing it below 3.5 °C. Furthermore, it is likely that many inceptions are triggered during storm events which vertically mix up cold deep waters to the surface layer (the storm season starts in autumn in the Baltic Sea). Thus, the mean thermal heat content of the previous summer and co-occurring atmospheric conditions in late autumn likely control the timing of inceptions more directly. Overall, the mean inception moves from day 113 (Fig. 6b) in the historical period to day 122, 126, 130, and 141 in the GWL1.5, GWL2.0, GWL3.0, and GWL4.0 scenarios respectively. Hence, the difference between GWL1.5 and 3.0 amounts to roughly ~one week, but a further warming to GWL4.0 would delay the winter inception by one additional week. Winter inception in the Greifswald Bay occurs generally a few days earlier, but the climate effect is similar (Fig. 6b, left panel).

3.5.1. Thermal threshold index

The THI (i.e. the total number of days >16 °C between March and June) is shown in Fig. 8 (upper panel). To extract the climate signal from inter-annual variability, 10-year running means are shown (black lines, Fig. 8). As an indicator for the models' internal inter-annual variability the 10-year running standard deviations are shown as shaded area around the mean. In each of the four models, the THI index increases towards the end of the 21st century. However, the individual models' internal variability can be fairly large. For RCO-MPI-ESM-LR the signal at the end of the 21st century only slightly exceed the noise level compared to the end of the 20th century, whereas the climate signal in RCO-EC-Earth and RCO-HadGEM2-ES models is quite strong. Depending on the model, the THI increases at the end of the century by 5 days (RCO-MPI-ESM), 20 days (RCO-EC-Earth), 20 days (RCO-IPSL-CMA5-MR), or 23 days (RCO-HadGEM2-ES), yielding a cross-ensemble average of ~17 days.

Not only the total number of days with temperatures ≥16 °C increases, but these days likewise occur earlier in the year. Figure (lower panel) shows the first occurrence averaged over entire spawning area. In the last two decades of the 20th century, the season with $T \geq 16$ °C start between day ~110 and day 115 (25. - 30. April) on average. Although also here the inter-annual variability (expressed as 10-year running standard deviation in Figure) is quite large the climate induced tendency towards an earlier onset is obvious. Hence, depending on the model, the season starts on average 7 days (RCO-MPI-ESM), 17 days (RCO-EC-Earth), 18 days (RCO-IPSL-CMA5-MR), or 13 days (RCO-HadGEM2-ES) earlier between 2090 and 2099 compared to 1976–2005 which yields an ensemble average of ~14 days.

4. Summary and conclusions

This study investigated SSTs and MHWs in the Baltic Sea and their potential adverse effects on the early herring life stages in the WBS. In order to assess future GWLs compliant with the Paris 2015 targets this study employed the transient climate scenario RCP85. The differences of RCP85 to other more mitigated scenarios like e.g. RCP45 for the first half of the 21st century are only moderate and we would expect uncertainties for our results with respect to the chosen scenario rather low. On the other hand the assessment of GWL1.5, and GWL2.0. GWL3.0 and GWL4.0 may not be reached in each of the ensemble models when choosing e.g. RCP45 or even RCP26. The results demonstrate already at the GWL1.5 a considerable mean warming of the Baltic Sea sea surface by 0.89 °C and by 0.83 °C for the shallow areas of WBS herring spawning grounds. With regard to MHWs, a GWL1.5 or GWL2.0 increases the average duration by 50 % or 100 % and the spatial extent is increases by the 3-fold or 4-fold (Fig. 3). Thus already in the mitigated scenarios compliant with the PA a substantial impact on ecosystem habitats can be expected with further cascading effects on other abiotic ecosystem drivers. For example, Safonova et al. (2024) recently demonstrated that MHWs can induce oxygen deficiencies in the coastal zone already under present climate conditions. More and more, the vulnerability of key marine species to MHWs becomes apparent. Prominent examples are the starfish *Asteria rubens* (Rühmkorff et al., 2023) and the seagrass *Zostera marina* (Wolf et al., 2022). The first is considered a key predator in the Baltic Sea while the seagrass transfers huge amounts of carbon and nutrients to the sediments, and thus, provides an important ecosystem service to mitigate the effect of anthropogenic carbon emissions and eutrophication (Röhr et al., 2018). Nevertheless, our study likewise demonstrates a significant mitigation effect for the MHW impact, if global warming remains compliant with GWL1.5 or even below GWL2.0. Hence, the yearly sum of MHW days is projected to increase by ~36–48 days with every additional 0.5 °C GWL step beyond GWL1.5.

In regard to phenological disturbances of early herring life stages in the WBS, this study found that the winter season will be substantially altered by the future GWL. In the high end GWL3.0, and GWL4.0 scenarios we found the winter termination on average 2 weeks earlier in the year, and the winter inception delayed by more than ~3 weeks (GWL3.0) or 4 weeks (GWL4.0) compared to the historical period (Fig. 6b, c). As a result, the winter length is nearly halved in the scenarios beyond the PA. In particular the probability for extreme winters increases. Most striking are the increases in missed winters, i.e. when the temperature does not fall below the herring initial spawning temperature. While those conditions are virtually absent in the historical climate, the share of missed winters increases from 9.3 % (GWL1.5) to 18.4 % (GWL2.0), 36.4 % (GWL3.0) 69.7 % at GWL4.0. In the remaining winters the probability for extreme early/late inceptions/terminations increases. For example, at GWL4.0 the likelihood inceptions occurring 40 days or later is 20 %. whereas in the historical period this likelihood is below 1 %. Analogously, the likelihood for terminations occurring earlier than 1 month compared to the average termination (24. March) is only 16 % in the historical period but increases to 30 % at GWL4.0. This is mainly attributed to more and longer MHWs in the high end GWL scenarios. Generally, the role of MHWs on winter timing is restricted to terminations which occur considerably earlier in the presence of MHWs compared to normal conditions without MHWs (Fig. 7a,b).

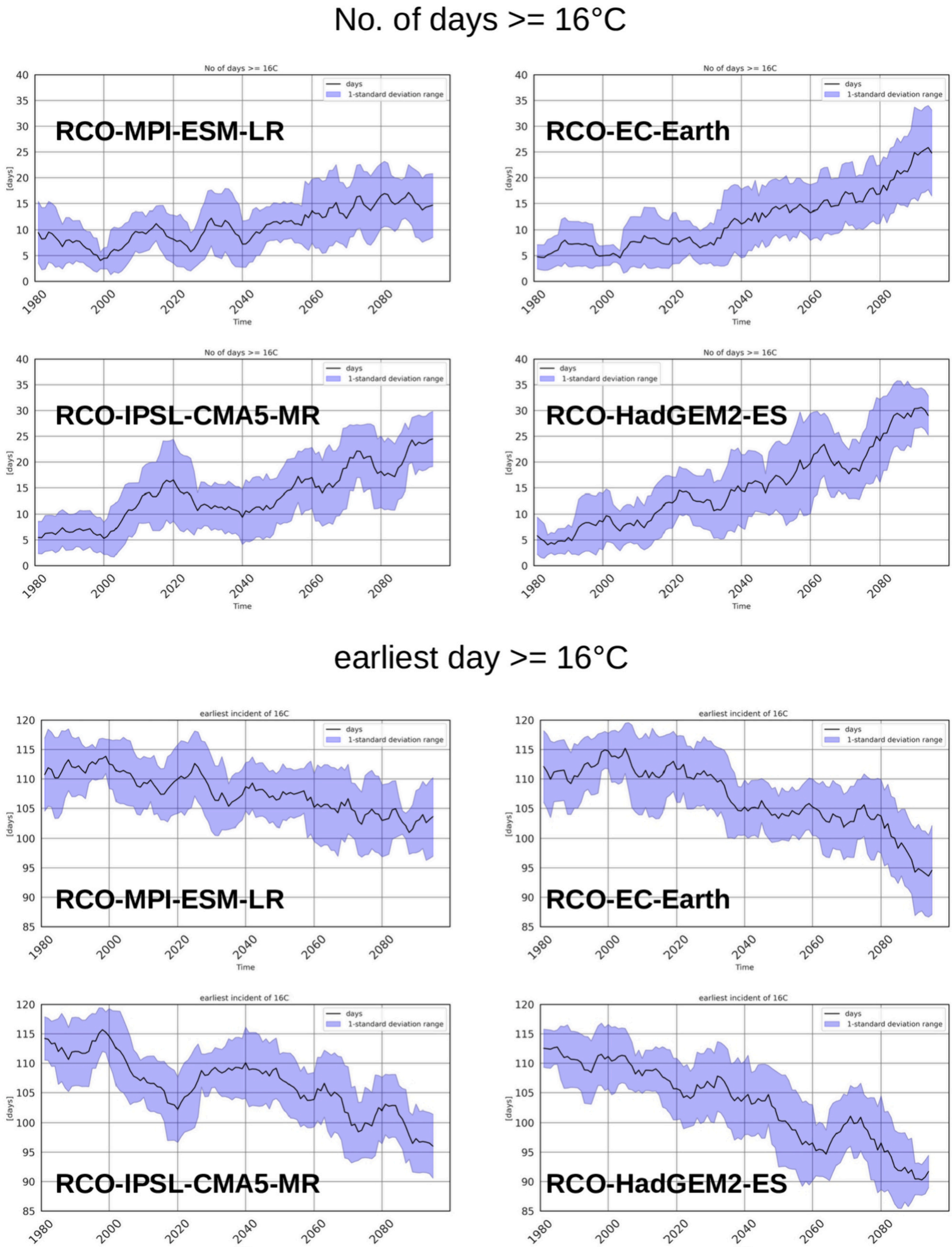

Fig. 8. Analysis of the THI index, i.e. No. of days >16 °C between March and June. Upper panel: yearly spawning-area averaged number of days with water temperatures ≥ 16 °C in the period March to June. Lower panel: yearly spawning-area averaged earliest occurrence (expressed as calendar day of year starting from 1. January) of water temperature ≥ 16 °C. Displayed are 10-year running averages (black lines) together with the 10-year running standard deviations centered around the mean (shaded). The results refer to climate scenario RCP85.

However, another important result of this study is the extraordinary high inter-annual variability in winter inceptions/terminations which is indicated by the large standard deviations in most of the considered herring indices (Fig. 6). The high variability very likely reflects the different phases of the North Atlantic Oscillation (NAO) which controls the heat supply from the Atlantic via the westerly wind regime during winter. This implies that the WBS herring population is already used to a high amplitude variations in winter timing which may help to better cope with projected future conditions. Furthermore, we note, that the knowledge about the mechanisms of how exactly phenological disturbances translate into corresponding reproductive failures is still lacking and so far based on empirical evidence. In the Northeast Atlantic, herring currently has its' distribution center in the temperate waters with the southernmost distribution in the northern Bay of Biscay (www.fishbase.org; last access 07/22/2024, Froese and Pauly, 2024). However, there the major herring stocks are winter spawners (in contrast to the WBS where they spawn in spring) and would leave the area during the summer month. In future warming scenarios it is currently unclear how western Baltic Sea herring stocks will respond. They could potentially stop returning from their North Sea feeding grounds but move northward to Scandinavian waters. An alternative hypothesis is as the spring spawning population in the Baltic Sea declines, autumn spawners may profit from mild winters and the herring population structure will shift in this direction. However, on climate time scales, it remains unclear whether or not the herring population could keep pace with the phenological disturbances projected by this study.

Besides, the changes in winter timing, this study likewise explored the effect of the mean GWL on the thermal threshold index as a proxy for herring larvae growth rates and healthy cardiac function (Moyano et al., 2020). We found a clear trend towards higher indices along with global warming and earlier occurrence of days >16 °C, which indicates an additional stress factor for the WBS Herring stock's reproduction success in a future warmer climate.

In this study we defined MHWs based on the historical climatology. This implies that the diagnosed changes in herring phenology and MHWs are probably mainly the result to the thermodynamic effect of climate change, i.e. the longer term trends of water mass warming (see e.g. Amaya et al., 2023) rather than in terms of dynamical changes in extremes in sensu stricto. To disentangle these two effects was not the purpose of this study and could be assessed by repeating the analysis using a definition of MHWs based on the climatologies of the individual GWLs separately.

Finally, in the Baltic Sea we can conclude that limiting global warming compliant with the PA can considerably mitigate the expected adverse effects on the marine ecosystem, though not completely eliminate them. Hence, the considered MHW indices (Fig. 3) and likewise the missed winter and winter duration (Fig. 6,d) indices are impacted already profoundly under the PA compliant GWLs. State of the art climate change assessments (Meier et al., 2022a) together with climate reconstructions (Luterbacher et al., 2016) suggest that the Baltic Sea may soon exceed the warming level of any previous natural climate oscillation during the past thousand years. Therefore, the projected changes in winter climate suggest that the Baltic Sea ecosystem will soon experience thermal conditions, that are unprecedented since at least the end of Medieval Warm Period, i.e. the latest warm anomaly related to natural variability. Therefore, in order to estimate concrete impacts on the future marine ecosystem from model projections, more research on species-specific environmental indicators, such as those used here for herring phenology, is urgently needed. Finally, our results suggest to consider climate change in managing fish stocks and coastal habitats.

CRediT authorship contribution statement

Matthias Gröger: Writing – review & editing, Writing – original draft, Visualization, Resources, Methodology, Investigation, Formal analysis, Conceptualization. **Florian Börgel:** Writing – review & editing, Conceptualization. **Sven Karsten:** Visualization, Resources. **H.E. Markus Meier:** Writing – review & editing, Conceptualization. **Kseniia Safonova:** Writing – review & editing. **Cyril Dutheil:** Writing – review & editing, Writing – original draft, Conceptualization. **Aurore Receveur:** Writing – review & editing, Visualization, Conceptualization. **Patrick Polte:** Writing – review & editing, Conceptualization.

Declaration of competing interest

The authors declare that they have no known competing financial interests or personal relationships that could have appeared to influence the work reported in this paper.

Data availability

Data will be made available on request.

Acknowledgements

The research presented in this study is part of the Baltic Earth program (Earth System Science for the Baltic Sea region, see https://www.baltic-earth.eu). This research was part-funded by the German Federal Ministry of Education and Research under grant number 03F0911A-K, project Coastal Futures. PP received funds by the EU-Data Collection Framework. AR is part of the MAESTRO project co-funded by the CESAB of the French Foundation for Research on Biodiversity (FRB) and FFP (France Filière Pêche). The responsibility for the content of this publication lies with the authors. This study has been conducted using E.U. Copernicus Marine Service Information; doi:10.48670/moi-00156.

Appendix A. Supplementary data

Supplementary data to this article can be found online at https://doi.org/10.1016/j.scitotenv.2024.175756.

References

Amaya, D.J., Jacox, M.G., Fewings, M.R., Saba, V.S., Stuecker, M.F., Rykaczewski, R.R., Ross, A.C., Stock, C.A., Capotondi, A., Petrik, C.M., Bograd, S.J., Alexander, M.A., Cheng, W., Hermann, A.J., Kearney, K.A., Powell, B.S., Apr 2023. Marine heatwaves need clear definitions so coastal communities can adapt. Nature 616 (7955), 29–32. https://doi.org/10.1038/d41586-023-00924-2 (PMID: 37012469).

Chauhan, A., Smith, P.A.H., Rodrigues, F., Christensen, A., St. John, M., Mariani, P., 2023. Distribution and impacts of long-lasting marine heat waves on phytoplankton biomass. Front. Mar. Sci. 10, 1177571 https://doi.org/10.3389/fmars.2023.1177571.

Christensen, O.B., Kjellström, E., Dieterich, C., Gröger, M., Meier, H.E.M., 2022. Atmospheric regional climate projections for the Baltic Sea region until 2100. Earth Syst. Dynam. 13, 133–157. https://doi.org/10.5194/esd-13-133-2022.

Dieterich, C., Wang, S., Schimanke, S., Gröger, M., Klein, B., Hordoir, R., Samuelsson, P., Liu, Y., Axell, L., Höglund, A., Meier, H.E.M., 2019. Surface heat budget over the North Sea in climate change simulations. Atmosphere 10, 272. https://doi.org/10.3390/atmos10050272.

Dutheil, C., Meier, H.E.M., Gröger, M., Börgel, F., 2022. Understanding past and future sea surface temperature trends in the Baltic Sea. Clim. Dyn. 58, 3021–3039. https://doi.org/10.1007/s00382-021-06084-1.

Dutheil, C., Meier, H.E.M., Gröger, M., Börgel, F., 2023. Warming of Baltic Sea water masses since 1850. Clim. Dyn. 61, 1311–1331. https://doi.org/10.1007/s00382-022-06628-z.

Fey, D., Pawelczyk, A., Woźniczka, A., 2014. Abundance and distribution of larval herring, Clupea harengus (Actinopterygii: Clupeiformes: Clupeidae) in the Pomeranian Bay, Baltic Sea as an indicator of spawning sites. Acta Ichthyol. Piscat. 44, 309–317. https://doi.org/10.3750/AIP2014.44.4.05.

Froese, R., Pauly, D., 2024. FishBase, World Wide Web electronic publication. www.fishbase.org (version (02/2024)).

Goebeler, N., Norkko, A., Norkko, J., 2022. Ninety years of coastal monitoring reveals baseline and extreme ocean temperatures are increasing off the Finnish coast. Commun. Earth Environ. 3, 215. https://doi.org/10.1038/s43247-022-00545-z.

Gröger, J.P., Hinrichsen, H.-H., Polte, P., 2014. Broad-scale climate influences on spring-spawning herring (*Clupea harengus*, L.) recruitment in the western Baltic Sea. PLoS One 9 (2), e87525. https://doi.org/10.1371/journal.pone.0087525.

Gröger, M., Arneborg, L., Dieterich, C., Höglund, A., Meier, H.E.M., 2019. Summer hydrographic changes in the Baltic Sea, Kattegat and Skagerrak projected in an ensemble of climate scenarios downscaled with a coupled regional ocean–sea

ice–atmosphere model. Clim. Dyn. 53, 5945–5966. https://doi.org/10.1007/s00382-019-04908-9.
Gröger, M., Placke, M., Meier, H.E.M., Börgel, F., Brunnabend, S.-E., Dutheil, C., Gräwe, U., Hieronymus, M., Neumann, T., Radtke, H., Schimanke, S., Su, J., Väli, G., 2022. The Baltic Sea Model Intercomparison Project (BMIP) – a platform for model development, evaluation, and uncertainty assessment. Geosci. Model Dev. 15, 8613–8638. https://doi.org/10.5194/gmd-15-8613-2022.
Gröger, M., Dutheil, C., Börgel, F., Meier, H.E.M., 2024. Drivers of marine heatwaves in a stratified marginal sea. Clim. Dyn. 7062 https://doi.org/10.1007/s00382-023-07062-5.
Hobday, A.J., Alexander, L.V., Perkins, S.E., Smale, D.A., Straub, S.C., Oliver, E.C., Benthuysen, J.A., Burrows, M.T., Donat, M.G., Feng, M., et al., 2016. A hierarchical approach to defining marine heatwaves. Prog. Oceanogr. 141, 227–238.
Hobday, A.J., Oliver, E.C., Gupta, A.S., Benthuysen, J.A., Burrows, M.T., Donat, M.G., Holbrook, N.J., Moore, P.J., Thomsen, M.S., Wernberg, T., et al., 2018. Categorizing and naming marine heatwaves. Oceanography 31 (2), 162–173.
Kjellström, E., Nikulin, G., Strandberg, G., Christensen, O.B., Jacob, D., Keuler, K., Lenderink, G., van Meijgaard, E., Schär, C., Somot, S., Sørland, S.L., Teichmann, C., Vautard, R., 2018. European climate change at global mean temperature increases of 1.5 and 2 °C above pre-industrial conditions as simulated by the EURO-CORDEX regional climate models. Earth Syst. Dynam. 9, 459–478. https://doi.org/10.5194/esd-9-459-2018.
Kuliński, K., Rehder, G., Asmala, E., Bartosova, A., Carstensen, J., Gustafsson, B., Hall, P. O.J., Humborg, C., Jilbert, T., Jürgens, K., Meier, H.E.M., Müller-Karulis, B., Naumann, M., Olesen, J.E., Savchuk, O., Schramm, A., Slomp, C.P., Sofiev, M., Sobek, A., Szymczycha, B., Undeman, E., 2022. Biogeochemical functioning of the Baltic Sea. Earth Syst. Dynam. 13, 633–685. https://doi.org/10.5194/esd-13-633-2022.
Luterbacher, J., Werner, J.P., Smerdon, J.E., Fernández-Donado, L., González-Rouco, F. J., Barriopedro, D., Ljungqvist, F.C., Büntgen, U., Zorita, E., Wagner, S., Esper, J., McCarroll, D., Toreti, A., Frank, D., Jungclaus, J.H., Barriendos, M., Bertolin, C., Bothe, O., Brázdil, R., Camuffo, D., Dobrovolný, P., Gagen, M., García-Bustamante, E., Ge, Q., Gómez-Navarro, J.J., Guiot, J., Hao, Z., Hegerl, G.C., Holmgren, K., Klimenko, V.V., Martín-Chivelet, J., Pfister, C., Roberts, N., Schindler, A., Schurer, A., Solomina, O., von Gunten, L., Wahl, E., Wanner, H., Wetter, O., Xoplaki, E., Yuan, N., Zanchettin, D., Zhang, H., Zerefos, C., 2016. European summer temperatures since Roman times. Environ. Res. Lett. 11, 024001 https://doi.org/10.1088/1748-9326/11/2/024001.
Meier, H.E.M., Dieterich, Gröger, M., 2021. Natural variability is a large source of uncertainty in future projections of hypoxia in the Baltic Sea. Commun. Earth Environ. 2, 50. https://www.nature.com/articles/s43247-021-00115-9 (2021).
Meier, H.E.M., Kniebusch, M., Dieterich, C., Gröger, M., Zorita, E., Elmgren, R., Myrberg, K., Ahola, M.P., Bartosova, A., Bonsdorff, E., Börgel, F., Capell, R., Carlén, I., Carlund, T., Carstensen, J., Christensen, O.B., Dierschke, V., Frauen, C., Frederiksen, M., Gaget, E., Galatius, A., Haapala, J.J., Halkka, A., Hugelius, G., Hünicke, B., Jaagus, J., Jüssi, M., Käyhkö, J., Kirchner, N., Kjellström, E., Kulinski, K., Lehmann, A., Lindström, G., May, W., Miller, P.A., Mohrholz, V., Müller-Karulis, B., Pavón-Jordán, D., Quante, M., Reckermann, M., Rutgersson, A., Savchuk, O.P., Stendel, M., Tuomi, L., Viitasalo, M., Weisse, R., Zhang, W., 2022a. Climate change in the Baltic Sea region: a summary. Earth Syst. Dynam. 13, 457–593. https://doi.org/10.5194/esd-13-457-2022.
Meier, H.E.M., Dieterich, C., Gröger, M., Dutheil, C., Börgel, F., Safonova, K., Christensen, O.B., Kjellström, E., 2022b. Oceanographic regional climate projections for the Baltic Sea until 2100. Earth Syst. Dynam. 13, 159–199. https://doi.org/10.5194/esd-13-159-2022.
Möllmann, C., Cormon, X., Funk, S., Otto, S., Schmidt, J., Schwermer, H., Sguotti, C., Voss, R., Quaas, M., 2021. Tipping point realized in cod fishery. Sci. Rep. 11 https://doi.org/10.1038/s41598-021-93843-z.
Moss, R.H., Edmonds, J.A., Hibbard, K.A., Manning, M.R., Rose, S.K., van Vuuren, D.P., Carter, T.R., Emori, S., Kainuma, M., Kram, T., Meehl, G.A., Mitchell, J.F.B., Nakicenovic, N., Riahi, K., Smith, S.J., Stouffer, R.J., Thomson, A.M., Weyant, J.P., Wilbanks, T.J., 2010. The next generation of scenarios for climate change research and assessment. Nature 463, 747–756. https://doi.org/10.1038/nature08823.
Moyano, M., Illing, B., Polte, P., Kotterba, P., Zablotski, Y., Gröhsler, T., Hüdepohl, P., Cooke, S., Peck, M., 2020. Linking individual physiological indicators to the productivity of fish populations: a case study of Atlantic herring. Ecol. Indic. 113, 106146 https://doi.org/10.1016/j.ecolind.2020.106146.
Moyano, M., Illing, B., Akimova, A., Alter, K., Bartolino, V., et al., 2023. Caught in the middle: bottom-up and top-down processes impacting recruitment in a small pelagic fish. Rev. Fish Biol. Fish. 33, 55–84. https://doi.org/10.1007/s11160-022-09739-2.
Placke, M., Meier, H.E.M., Gräwe, U., Neumann, T., Frauen, C., Liu, Y., 2018. Long-term mean circulation of the Baltic Sea as represented by various ocean circulation models. Front. Mar. Sci. 5, 287. https://doi.org/10.3389/fmars.2018.00287.
Polte, P., Gröhsler, T., Kotterba, P., von Nordheim, L., Moll, D., Santos, J., Rodriguez-Tress, P., Zablotski, Y., Zimmermann, C., 2021. Reduced reproductive success of western Baltic herring (*Clupea harengus*) as a response to warming winters. Front. Mar. Sci. 8, 589242 https://doi.org/10.3389/fmars.2021.589242.
Receveur, A., Bleil, M., Funk, S., Stötera, S., Gräwe, U., Naumann, M., Dutheil, C., Krumme, U., 2022. Western Baltic cod in distress: decline in energy reserves since 1977. ICES J. Mar. Sci.: J. Conseil 79, 1187–1201. https://doi.org/10.1093/icesjms/fsac042.
Reckermann, M., Omstedt, A., Soomere, T., Aigars, J., Akhtar, N., Bełdowska, M., Bełdowski, J., Cronin, T., Czub, M., Eero, M., Hyytiäinen, K.P., Jalkanen, J.-P., Kiessling, A., Kjellström, E., Kuliński, K., Larsén, X.G., McCrackin, M., Meier, H.E.M., Oberbeckmann, S., Parnell, K., Pons-Seres de Brauwer, C., Poska, A., Saarinen, J., Szymczycha, B., Undeman, E., Wörman, A., Zorita, E., 2022. Human impacts and their interactions in the Baltic Sea region. Earth Syst. Dynam. 13, 1–80. https://doi.org/10.5194/esd-13-1-2022.
Röhr, M.E., Holmer, M., Baum, J.K., Björk, M., Boyer, K., Chin, D., et al., 2018. Blue carbon storage capacity of temperate eelgrass (Zostera marina) meadows. Glob. Biogeochem. Cycles 32, 1457–1475. https://doi.org/10.1029/2018GB005941.
Rühmkorff, S., Wolf, F., Vaiedsamiei, J., Barboza, F.R., Hiebenthal, C., Pansch, C., 2023. Marine heatwaves and upwelling shape stress responses in a keystone predator. Proc. R. Soc. B. https://doi.org/10.1098/rspb.2022.2262.
Safonova, K., Meier, H.E.M., Gröger, M., 2024. Summer heatwaves on the Baltic Sea seabed contribute to oxygen deficiency in shallow areas. Commun. Earth Environ. 5, 106. https://doi.org/10.1038/s43247-024-01268-z.
Saraiva, S., Meier, H.E.M., Andersson, H., Höglund, A., Dieterich, C., Gröger, M., Hordoir, R., Eilola, K., 2018. Baltic Sea ecosystem response to various nutrient load scenarios in present and future climates. Clim. Dyn. 52, 3369–3387. https://doi.org/10.1007/s00382-018-4330-0.
Saraiva, S., Meier, H.E.M., Andersson, H., Höglund, A., Dieterich, C., Gröger, M., Hordoir, R., Eilola, K., 2019. Uncertainties in projections of the Baltic Sea ecosystem driven by an ensemble of global climate models. Front. Earth Sci. 6, 244. https://doi.org/10.3389/feart.2018.00244.
Sen Gupta, A., May 2023. Marine heatwaves: definition duel heats up. Nature 617 (7961), 465. https://doi.org/10.1038/d41586-023-01619-4 (PMID: 37193814).
UNFCCC: The Paris Agreement, 2015. United Nations framework convention on climate change. available at: http://unfccc.int/paris_agreement/items/9485.php (last access:).
Viitasalo, M., Bonsdorff, E., 2022. Global climate change and the Baltic Sea ecosystem: direct and indirect effects on species, communities and ecosystem functioning. Earth Syst. Dynam. 13, 711–747. https://doi.org/10.5194/esd-13-711-2022.
Wolf, F., Seebass, K., Pansch, C., 2022. The role of recovery phases in mitigating the negative impacts of marine heatwaves on the sea star Asterias rubens. Front. Mar. Sci. 8, 790241 https://doi.org/10.3389/fmars.2021.79024.